Dependence of the occupancy of excimer-forming conformations on the size of the flexible spacer in polyesters from terephthalic acid and mono-, di- or triethylene glycol

Francisco Mendicuti, Vellarkad N. Viswanadhan and Wayne L. Mattice
Department of Polymer Science, The University of Akron, Akron, Ohio 44325, USA
(Received 8 September 1987; revised 16 October 1987; accepted 16 October 1987)

Steady-state emission and excitation spectra have been measured for dimethyl terephthalate and three polyesters in four solvents. The polymers have the repeating unit AB_m, where A is $-CO-C_6H_4-COO-$, B is $-CH_2CH_2O-$ and $m=1$, 2 or 3. The solvents are dichloroethane, dioxane, ethyl acetate and cyclohexane. Excimer emission is seen in all three polymers. At 300 K, the ratio excimer to monomer emission is always largest in the polymer for which $m=2$. A rotational isomeric treatment of the unperturbed polymers identifies the conformations that should be conducive to excimer formation by nearest-neighbour aromatic rings. The population of such conformations is maximal in the polyester in which $m=2$.

(Keywords: polyester; chain conformation; excimer)

INTRODUCTION

The intramolecular formation of excimers is a common phenomenon in polymers that contain aromatic rings. In aryl vinyl polymers, excimer formation is often dominated by pairs of aromatic rings that are nearest neighbours in the polymer chain[1,2]. However, there is not an absolute requirement that the rings involved in excimer formation must be bonded to main-chain atoms i and $i+2$. A well known exception is provided by excimer formation with the acenaphthalene unit[3], which has unusual steric requirements. Intramolecular pyrene excimer formation in polystyrene chains end-labelled with pyrene clearly shows that groups far removed from one another in the fully extended chain can participate in the formation of the excited-state complex when the chain adopts certain less extended conformations[4]. In the end-labelled polystyrenes examined by Winnik, the extent of excimer formation decreases as the polystyrene segment becomes of higher molecular weight. This behaviour is expected because the probability for cyclization is proportional to $n^{-3/2}$ in long freely jointed chains of n bonds[5].

Rotational isomeric state models for unperturbed chain molecules also predict that the probability for cyclization will become proportional to $n^{-3/2}$ in the limit as n becomes infinite. However, at smaller n the restrictions imposed by bond angles, rotational potentials and short-range interactions can produce marked departure from the limiting $n^{-3/2}$ behaviour. Indeed, there are well known chains, such as poly(dimethylsiloxane), where the macrocyclization equilibrium constants pass through local maxima and minima at finite n[6,7]. For this reason, it can be expected that certain polymers of the form $(AB_m)_x$, where A contains a potentially excimer-forming aryl unit and B is a flexible spacer, will exhibit an extent of excimer emission that is not necessarily a monotonic function of m. Here we describe the data that show that maximal excimer emission in dilute solution can be obtained at $m=2$ when A is $-CO-C_6H_4-COO-$ and B is $-CH_2-CH_2-O-$. A preliminary account was presented earlier[8]. A rotational isomeric state analysis provides supporting evidence that excimer-forming conformations are more frequently populated when $m=2$ than when $m=1$ or 3.

EXPERIMENTAL DETAILS

The chains studied are polyesters of terephthalic acid and $HO(CH_2CH_2O)_mH$, $m=1$, 2 or 3. Dimethyl terephthalate (Merck) was used as a model compound. The samples in which $m=2$ and 3 were prepared and purified in the manner described earlier[9,10]. Poly(ethylene terephthalate) was purchased from Aldrich, purified by reprecipitation three times with methanol from phenol solution, and dried *in vacuo* at 75°C to eliminate phenol. Dichloroethane, dioxane, ethyl acetate and cyclohexane were purchased from Aldrich (spectrophotometric grade) and used without further purification. Fluorescence measurements were performed with an SLM 8000C fluorimeter equipped with a double excitation monochromator. Slits were 8 nm for excitation and 8 nm for emission. Magic-angle conditions were employed. Solvent blanks were measured and subtracted from the observed spectra. Typical absorbances at the wavelength of excitation were 0.01 (cyclohexane, 286 nm), 0.10 (dichloroethane, 286 nm), 0.12 (dioxane, 270 nm) and 0.04 (ethyl acetate, 286 nm).

EXPERIMENTAL RESULTS

Figure 1 depicts emission spectra observed upon excitation at 286 nm in dichloroethane for dimethyl terephthalate and the polyester in which $m=2$. Dimethyl terephthalate has a single emission band at 324 nm, similar to that reported upon excitation at 260 nm[11], and the intensity decreases as the temperature increases. Emission by the polymer also decreases in intensity with increasing temperature, but the emission band is much broader, with substantial intensity far to the red of the

0032-3861/88/050875-05$03.00

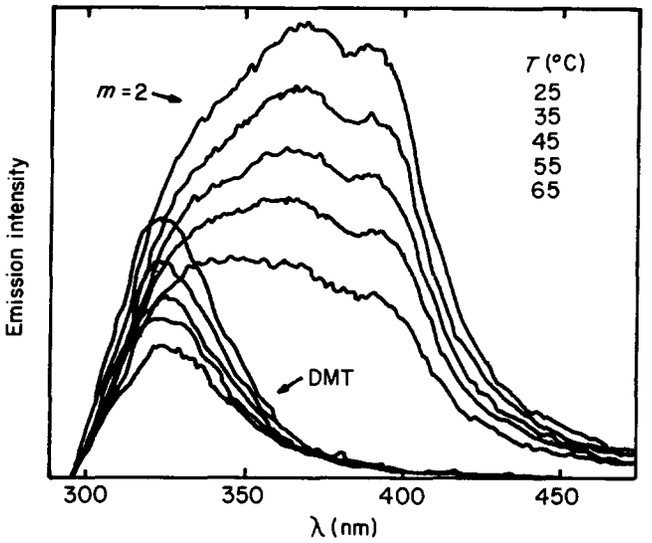

Figure 1 Emission spectra for dimethyl terephthalate (DMT) and the polyester with $m=2$ upon excitation at 286 nm in dichloroethane. The scaling for dimethyl terephthalate intensity vs. polymer intensity is arbitrary

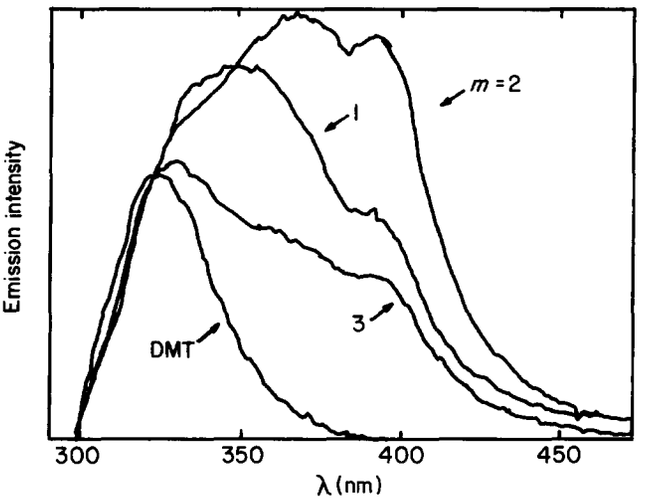

Figure 2 Emission spectra for dimethyl terephthalate and three polyesters in dichloroethane at 25°C. Spectra are normalized to the same intensity at 324 nm

emission by dimethyl terephthalate[11]. Excitation spectra are similar for both materials in dilute solution, and the excitation spectrum for the polymer is the same for emission at 324 and 390 nm. The emission spectra for the polymer and model compound in dilute solution do not change shape upon small changes in the wavelength of excitation. The change in the shape of the emission band upon incorporation of the chromophore into the polymer is attributed to excimer formation in the macromolecule.

The data from *Figure 1* at 25°C are combined in *Figure 2* with similar data for the polyesters in which $m=1$ and 3. The four spectra are normalized to the same intensity at 324 nm, which is the location of the emission maximum for dimethyl terephthalate. In the absence of this normalization, the polymer with the most intense emission is poly(ethylene terephthalate). Fluorescence quantum yields in dichloroethane are approximately 0.019, 0.006 and 0.004 for the polyesters with $m=1$, 2 and 3, respectively. *Figure 2* shows that the ratio of the intensity of excimer emission, I_D, to the intensity of monomer emission, I_M, does *not* experience a monotonic decrease upon increasing the number of ethylene oxide units between the aromatic rings. The maximum in I_D/I_M is obtained in the polyester in which $m=2$.

Figure 2 shows that dimethyl terephthalate has very little emission at 390 nm, but all three polymers exhibit appreciable emission at this wavelength. Upon adoption of 324 and 390 nm for measurement of I_M and I_D, respectively, the behaviour of I_D/I_M as a function of temperature in dichloroethane is depicted in *Figure 3*. The polyester in which $m=2$ has the largest I_D/I_M at 25°C, but its domination of the polymer in which $m=1$ decreases as the temperature rises. These two polymers have equal I_D/I_M at about 60°C. The polymer in which $m=3$ has the smallest I_D/I_M at all temperatures studied.

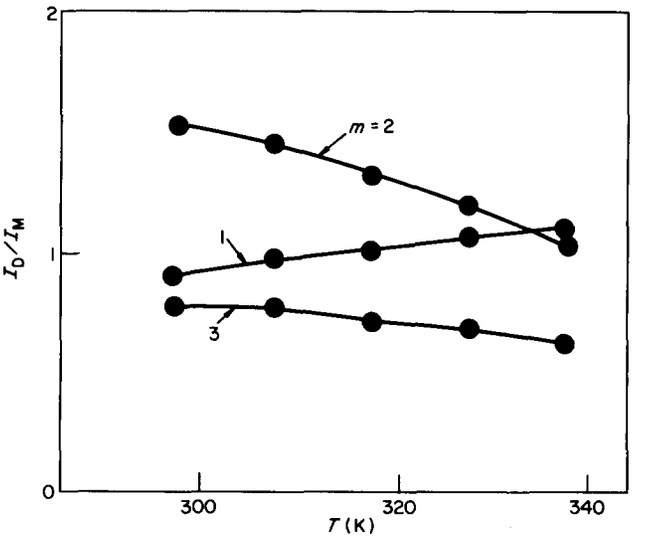

Figure 3 I_D/I_M as a function of temperature in dichloroethane for the polyesters

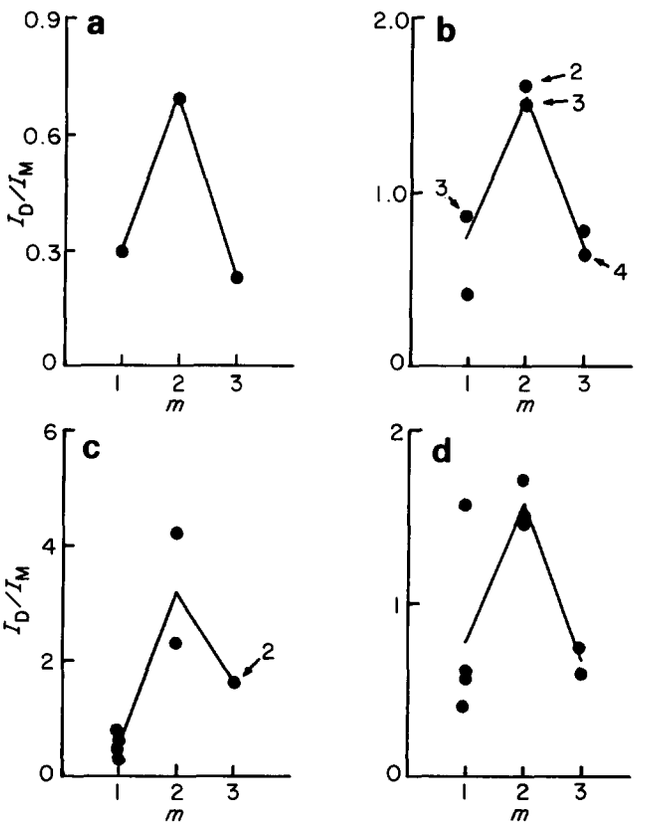

Figure 4 I_D/I_M for the three polyesters at 25°C in (a) cyclohexane, (b) dichloroethane, (c) ethylacetate and (d) dioxane. Points that denote essentially identical results from multiple measurements are denoted by an arrow and the number of measurements

Measurements were performed in other solvents at 25°C in order to ascertain whether the relationship between I_D/I_M and m is peculiar to the polymers in dichloroethane. *Figure 4* depicts I_D/I_M in dichloroethane, cyclohexane, dioxane and ethyl acetate. The full lines connect the averages of the I_D/I_M for the three polymers. In all four solvents, the largest I_D/I_M is clearly the sample in which $m=2$. The highest point for $m=1$ in the panel for dioxane was the only data point available in this solvent for the polymer in which $m=1$ at the time of preparation of the preprint[8]. As shown in *Figure 4*, three subsequent determinations give significantly smaller values of I_D/I_M.

ROTATIONAL ISOMERIC STATE METHODS

The objectives of the rotational isomeric state analysis are identification of the conformations of $-(CH_2CH_2O)_m-$ that are conducive to excimer formation by the aromatic rings at either end of this fragment and the evaluation of the probability of occupancy of these conformations in chains unperturbed by long-range interactions. The rotational isomeric state models used are minor adaptations of those developed for treatment of the unperturbed polyesters[9,10]. They have been shown to provide an adequate description of the mean-square dipole moment[9,10], optical configuration parameter[10] and molar Kerr constant[12] for members of this series. The fragment of interest for present purposes is depicted in *Figure 5*. Its configuration partition function, Z_m, is formulated in terms of the statistical weight matrices $U_[$, $U(\sigma,\omega)$ and $U_]$ as:

$$Z_m = U_[U(\sigma_\eta,\omega_{k\eta})[U(\sigma'',\omega)U(\sigma'',\omega_0)U(\sigma_\eta,\omega)]^{m-1} \times U(\sigma_k,\omega_{k\eta})U_] \quad (1)$$

where

$$U_[= [1 \quad \sigma_k \quad \sigma_k] \quad (2)$$

$$U(\sigma,\omega) = \begin{bmatrix} 1 & \sigma & \sigma \\ 1 & \sigma & \sigma\omega \\ 1 & \sigma\omega & \sigma \end{bmatrix} \quad (3)$$

$$U_] = \begin{bmatrix} 1 \\ 1 \\ 1 \end{bmatrix} \quad (4)$$

The following energies (in kcal mol^{-1}) are used for calculation of the statistical weights: $E_{\sigma k}=0.424$, $E_{\sigma''}=0.927$, $E_{\omega k\eta}=1.410$, $E_\omega=0.355$ and $E_{\omega 0}=\infty$. The calculations reported here employ $E_{\sigma\eta}=-0.4$ kcal mol^{-1}, which is the value obtained by Abe and Mark[13]. The model assumes standard bond lengths and angles, with the dihedral angles of *gauche* states located $\pm 120°$ from the dihedral angle for the *trans* state.

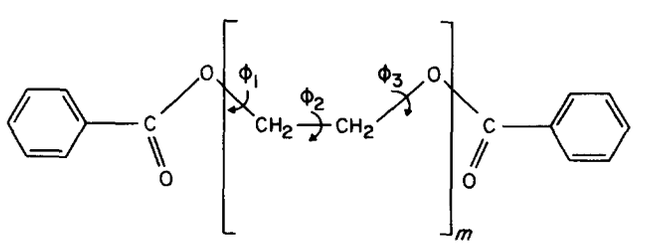

Figure 5 Bonds about which rotation occurs in the rotational isomeric state treatment

The assumed target conformation (excimer-forming conformation) has the two rings depicted in *Figure 5* oriented so that the normals to their planes are parallel to one another, the centres of the two rings are 0.35 nm apart and the line joining the centres is parallel to the normals. However, since the use of rotational isomeric state (RIS) models does not continuously sample conformational space, but instead examines this space at judiciously selected intervals, some tolerance must be provided in the target geometry.

The RIS model chains are generated by the procedure of discrete enumeration. Fragments with $m=1$, 2 or 3 are generated with three states, namely *trans* (t), *gauche*$^+$ (g^+) and *gauche*$^-$ (g^-), for the bonds about which rotation occurs. This procedure assigns 3^{3m} conformations to each fragment. This set of conformations is enlarged by allowing for excursions of the variable dihedral angles from the one value that is often associated with a particular rotational isomer. The size of the excursion is denoted by $\Delta\phi$. Each bond rotation at a well can assume any one of three dihedral angles, i.e. $\phi_r-\Delta\phi$, ϕ_r and $\phi_r+\Delta\phi$, where ϕ_r is 180° for t and $\pm 60°$ for $g^\pm$. The value of $\Delta\phi$ is taken to be 20°, which is sufficient to produce a torsional energy larger than that at the minimum by an amount slightly greater than kT. The number of conformations allowed increases from 3^{3m} to 3^{6m} when $\Delta\phi$ changes from 0 to a value different from 0. The number of conformations examined was reduced by examination of only one member of each pair of mirror images (e.g. g^+tt and g^-tt in the case of $m=1$) and by assuming that at least one *gauche* placement is necessary for excimer formation. In this manner, the number of conformations to be examined is reduced from 3^{6m} to $(3^{6m}-3^{3m})/2$. The covalent structure is palindromic, but this source of redundancy is not eliminated in the $(3^{6m}-3^{3m})/2$ conformations.

The large number of conformations specified by $(3^{6m}-3^{3m})/2$ when $m=3$ prompted a modification in the procedure. Here the initial scan of the accessible geometries was made with $\Delta\phi=0$, thereby reducing the number of conformations examined to $(3^{3m}-1)/2$. The conformations that placed the two rings in the general vicinity of the target orientation were flagged, and each of these conformations was then examined in detail using $\Delta\phi=20°$. If a conformation was flagged in the initial scan, it prompted the generation of 3^{3m} conformations where each variable dihedral angle was independently assigned as $\phi_r-\Delta\phi$, ϕ_r or $\phi_r+\Delta\phi$. These 3^{3m} conformations were compared with the same criteria for excimer formation that were employed when $m=1$ or 2.

The criteria for excimer formation are determined heuristically: first the set of criteria that must be satisfied in order to produce an excimer when $m=1$ is determined. The same criteria are then used to examine the excimer formation when $m>1$. All chains are assumed to have the first ring in the xy plane, with the origin of the coordinate system at the centre of the ring. Each conformation is examined to ascertain whether (a) the normals to the rings are sufficiently close to a parallel arrangement, (b) the centres of the rings are close enough to a separation of 0.35 nm, and (c) the line joining the centres is parallel to the normals. This objective requires measurement of the angle between the planes of the two rings, the difference in z coordinates of the centres of the two rings and the separation in the xy plane of the centres of the two rings.

The oscillations of a dihedral angle between $\phi_r-\Delta\phi$

and $\phi_r+\Delta\phi$ will occur many times during the lifetime of the electronic excited state. It is assumed that these torsional oscillations are so rapid that the fragment will pass through the best excimer-forming geometry for a particular combination of wells, i.e. for a particular rotational isomer, during the lifetime of the electronic excited states. For this reason the classification of a particular rotational isomer as excimer-forming or non-excimer-forming is based on the optimal geometry obtained upon independent variation of the $3m$ dihedral angles over the range $\pm\Delta\phi$. The ratio of the statistical weight for a conformation to the configuration partition function gives the probability for occupancy of that conformation. The orientation of the two rings in each conformation is equivalent to the orientation seen in the mirror image (obtained by reversing the sign of all *gauche* states in the conformational sequence) and in the conformation obtained by reversing the whole sequence. Only one of these conformations is listed in the tables. The tabulated probability is obtained by multiplication of the statistical weight for a single conformation by I/Z, where $I=4$ for non-palindromic sequences and $I=2$ for palindromic sequences.

RESULTS OF THE ROTATIONAL ISOMERIC STATE ANALYSIS

The calculations pertain to 298 K. The conditions used are: maximum allowed angle between normals to the rings, 28°; difference in the z coordinates between the ring centres, 0.35 ± 0.05 nm; radial distance between the centres of the rings, 0.135 nm; and $\Delta\phi=20°$. These conditions provide sufficient tolerance so that an excimer-forming conformation is detected when $m=1$. This conformation is the triad of *gauche* placements of opposite sign ($g^{\pm}g^{\mp}g^{\pm}$) with dihedral angles $\pm80°$, $\mp40°$ and $\pm60°$. The statistical weight is $\sigma_k^2\sigma_\eta\omega_{k\eta}^2$, and the probability of occurrence of this conformation is 0.0006.

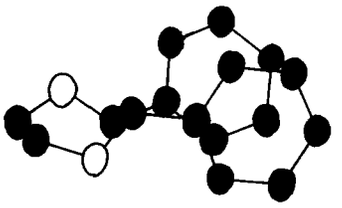

Figure 6 Ball-and-stick representation of the excimer geometry at $m=1$. Carbonyl oxygen atoms are omitted in the interest of clarity. Filled and open circles denote carbon and oxygen atoms, respectively

Table 1 Excimer-forming conformations when $m=2$

	Sequence	Statistical weight	Probability[a]
1.	$g^-g^-ttg^+g^+$	$\sigma_\eta^2\sigma_k^2$	0.01696
2.	$g^-g^-tg^-g^-t$	$\sigma_\eta^2\sigma_k\sigma''$	0.01448
3.	$g^-g^-g^-tg^-g^-$	$\sigma_k^2\sigma_\eta^2\sigma''$	0.00704
4.	$g^-g^+ttg^-t$	$\sigma_\eta^2\sigma_k\omega_{k\eta}$	0.00640
5.	$g^-ttg^+g^-t$	$\sigma_k\sigma_\eta\sigma''\omega$	0.00376
6.	$g^-g^-ttg^+g^-$	$\sigma_k^2\sigma_\eta^2\omega_{k\eta}$	0.00312
7.	$g^-g^+tg^+g^+t$	$\sigma_\eta^2\sigma_k\sigma''\omega_{k\eta}$	0.00132
8.	$tg^-g^+g^+tg^+$	$\sigma''^2\sigma_\eta\sigma_k\omega$	0.00080
9.	$g^-g^-tg^-g^-g^+$	$\sigma_k^2\sigma_\eta^2\sigma''\omega_{k\eta}$	0.00065
10.	$g^-g^-g^-tg^-g^+$	$\sigma_k^2\sigma_\eta^2\sigma''\omega_{k\eta}$	0.00065
11.	$g^-g^+g^-ttg^-$	$\sigma_k^2\sigma_\eta\sigma''\omega\omega_{k\eta}$	0.00012
12.	$g^-g^+g^+tg^+g^-$	$\sigma_\eta^2\sigma_k\sigma''\omega^2{}_{k\eta}$	0.00009
13.	$g^-g^+g^-g^-tg^-$	$\sigma_k^2\sigma''^2\sigma_\eta\omega\omega_{k\eta}$	0.00004

[a] $\Sigma p=0.05543$

Table 2 Dihedral angles forming the best excimers when $m=2$

	Sequence of dihedral angles (deg.)	Interplanar angle (deg.)
1.	60, 40, 180, −160, −40, −60	168.9
2.	80, 80, −160, 40, 60, 180	155.1
3.	40, 40, 80, 160, 40, 60	24.4
4.	80, −40, 180, −160, 40, 40	154.9
5.	80, −160, 180, −60, 60, −160	171.3
6.	40, 60, 160, 160, −60, 80	14.6
7.	80, −80, 160, −60, −80, 160	11.9
8.	160, 40, −60, −60, 160, −80	161.3
9.	40, 60, −160, 60, 80, −40	15.4
10.	60, 40, 40, 180, 60, −60	178.4
11.	80, −80, 60, 160, −160, 40	17.3
12.	80, −40, −80, −160, −60, 60	17.6
13.	60, −80, 80, 80, −160, 80	10.8
14.	60, 80, −80, −40, −160, 80	159.6
15.	160, −160, 60, −40, 80, 160	165.5
16.	40, 40, 60, −80, −80, 40	162.4
17.	180, 40, 80, −60, −80, 160	166.0
18.	40, −80, 40, −60, 160, 40	161.8
19.	−160, 80, 60, −40, −80, 40	15.2

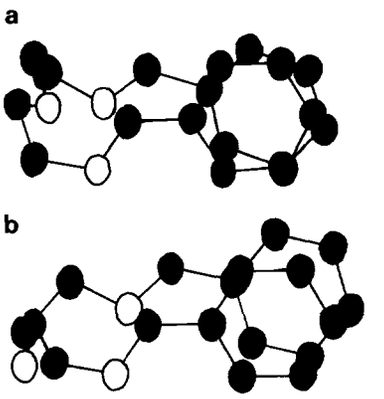

Figure 7 Ball-and-stick representation of (a) the dominant excimer geometry $m=2$, and (b) the second most dominant excimer in $m=2$

When the temperature is raised to 350 K, the probability increases to 0.0016. *Figure 6* shows the ball-and-stick representation.

In *Table 1*, the sequences of rotational states responsible for excimer geometries and their statistical weights, along with the probability of each sequence, are presented for $m=2$. The sum of the probabilities of all 13 sequences is 0.0554. Six other sequences are of zero probability owing to the presence of ω_0 in the statistical weight. Some sequences, such as the first in *Table 1*, are pseudo-palindromic (i.e. the inverse and mirror image of that sequence are identical). *Table 2* presents the set of dihedral angles which are among the best excimers for each sequence, along with the interplanar angle between the rings. The best excimers are those with the interplanar angle close to 0° or 180°. Two dominant conformers are depicted in *Figures 7a* and *7b*. Comparison of *Figures 6* and *7* shows that there is better overlap of the aromatic rings in the excimer-forming conformations in the polymer where $m=2$.

Table 3 lists the sequences of rotational states causing the excimer geometries, along with their statistical weights and probabilities, for the polymer when $m=3$. This is only a partial list, however. This list has been obtained by the modified algorithm described above, with the following relaxation. First the distance criterion (measured by the z coordinate of the terminal ring) is relaxed from 0.3–0.4 nm to 0–1 nm. Then, without

Table 3 Excimer-forming conformations when $m=3$

	Sequence[a]	Statistical weight	Probability[b]
1.	$g^-g^-ttg^-tg^-g^+t$	$\sigma_\eta^3\sigma_k\sigma''\omega$	0.00184
2.	$tg^+g^+tg^+tg^-g^-g^-$	$\sigma_\eta^3\sigma''^2\sigma_k$	0.00070
3.	$g^-g^-ttg^-g^+g^+g^-t$	$\sigma_\eta^3\sigma''^2\sigma_k\omega$	0.00038
4.	$tg^-ttg^-g^+g^+tt$	$\sigma_\eta^4\sigma''^2\omega$	0.00037
5.*	$g^-g^-g^-tg^-tg^-g^-g^-$	$\sigma_\eta^3\sigma''^2\sigma_k$	0.00035
6.*	$tg^-g^-tttg^-g^-t$	$\sigma_\eta^2\sigma''^2$	0.00034
7.	$g^-tg^+g^+g^-ttg^+t$	$\sigma_\eta^2\sigma''^2\sigma_k\omega$	0.00018
8.*	$g^-g^-g^+tg^+tg^+g^-g^-$	$\sigma_\eta^3\sigma_k^2\sigma''^2\omega^2$	0.00005

[a] Palindromes are marked with an asterisk
[b] $\Sigma p=0.00421$

Table 4 Dihedral angles forming the best excimers when $m=3$

	Sequence of dihedral angles (deg.)	Interplanar angle (deg.)
1.	80, 40, 160, −160, 60, −160, 80, −40, −160	2.8
2.	−160, −40, −80, 160, −40, −160, 60, 60, 80	3.8
3.	60, 80, −160, 180, 40, −60, −40, 60, 180	1.3
4.	80, 40, −60, 60, 80, 40, −40, 60, 60	1.5
5.	80, 60, 60, −160, 80, −160, 40, 60, 80	4.9
6.	160, 40, 60, −160, 160, 180, 80, 40, 160	1.4
7.	80, 180, −60, −60, 40, 160, −160, −40, 180	0.7
8.	80, 40, −40, 180, −60, 180, −40, 40, 80	19.1

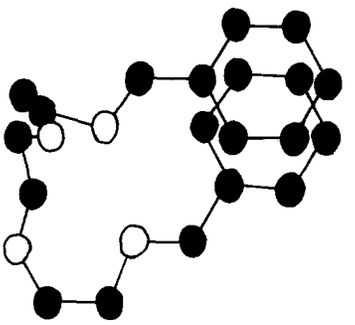

Figure 8 Ball-and-stick representation of the dominant excimer in $m=3$

allowing any tolerance in the dihedral angles used for the rotational states (i.e. setting $\Delta\phi$ to 0°), the set of conformational sequences satisfying the relaxed distance criterion and other criteria are obtained. From this set of conformational sequences, those satisfying the earlier criteria are taken when the tolerance in dihedral angles is reimposed to $\Delta\phi=20°$. The best excimers are presented in *Table 4*. *Figure 8* shows the dominant excimer in $m=3$.

The results clearly show that the probabilities for assumption of the target geometry in the unperturbed chains are of the order $(m=2)>(m=3)>(m=1)$. If all statistical weights were assigned a value of 1, thereby making all conformational sequences equally probable, the order would change to $(m=1)>(m=2)>(m=3)$. The reason why $m=2$ has the greatest probability of excimer formation becomes apparent upon examination of the statistical weights for the excimer geometries in the series. The presence of ω in their statistical weights is responsible for the low probabilities of many excimer geometries for $m=3$. The $m=1$ excimer also has a low probability because the statistical weight for $g^\pm g^\mp g^\pm$ placements has $\omega_{k\eta}^2$ in the weight, $\sigma_k^2\sigma_\eta\omega_{k\eta}^2$. In contrast, some $m=2$ excimers have higher probabilities due to the absence of ω in their statistical weights. These are the dominant excimers for $m=2$.

The results presented here apply to the fragment depicted in *Figure 5*. They should be appropriate for the formation of excimers between nearest-neighbour aromatic rings in the polymer. They do not include assessments of the consequence of intramolecular excimers of longer range or intermolecular excimers. The method used takes no account of any migration of excitation energy. Intrachain dynamics is included in a limited sense; there is provision for independent torsional oscillations within wells, but no allowance for jumps from one well to another during the lifetime of the electronic excited state. Nevertheless, the simple model does show that the polymer in which $m=2$ is the one with the greatest probability for occupancy of rotational isomers conducive to excimer formation by nearest-neighbour aromatic rings. This probability, however, is quite small, being about 0.07 at 300 K. The large ratio of excimer to monomer emission in the polymer suggests that there may be another mechanism for populating the excimer-forming state. This mechanism might be the jump during the lifetime of the excitation from one well to another, a process that may be subject to analysis by recent advances in rotational isomeric state theory[14].

ACKNOWLEDGEMENTS

This research was supported by National Science Foundation Grant DMR 86-96071 (WLM) and a NATO Fellowship (FM).

REFERENCES

1 Hirayama, F. *J. Chem. Phys.* 1965, **42**, 3163
2 deSchryver, F. C., Collart, P., Vandendriessche, J., Goedeweeck, R., Swinner, A. and Van der Auweraer, M. *Acct. Chem. Res.* 1987, **20**, 159
3 Wang, Y.-C. and Morawetz, H. *Makromol. Chem., Suppl.* 1975, **1**, 283
4 Winnik, M. A. *Acct. Chem. Res.* 1985, **18**, 73
5 Jacobson, H. and Stockmayer, W. H. *J. Chem. Phys.* 1950, **18**, 1600
6 Suter, U. W., Mutter, M. and Flory, P. J. *J. Am. Chem. Soc.* 1976, **98**, 5740
7 Semlyen, J. A. (Ed.), 'Cyclic Polymers', Elsevier, Barking, 1986
8 Mendicuti, F., Viswanadhan, V. N. and Mattice, W. L. *Polym. Prepr., Div. Polym. Chem., Am. Chem. Soc.* 1987, **28**(2), 82
9 Riande, E. *J. Polym. Sci., Polym. Phys. Edn.* 1977, **15**, 1397
10 Riande, E. and Guzman, J. *J. Polym. Sci., Polym. Phys. Edn.* 1985, **23**, 1235
11 Hemker, D. J., Frank, C. W. and Thomas, J. W. *Polym. Prepr., Div. Polym. Chem., Am. Chem. Soc.* 1986, **27**, 210
12 Mendicuti, F. and Saiz, E. *Polym. Bull.* 1984, **11**, 533
13 Abe, A. and Mark, J. E. *J. Am. Chem. Soc.* 1976, **98**, 6468
14 Bahar, I. and Erman, B. *Macromolecules* 1987, **20**, 1368